Journal of
Materials Chemistry A

Accepted Manuscript

This article can be cited before page numbers have been issued, to do this please use: R. Jayarajan, R. Kumar, J. Gupta, G. Dev, P. Kadu, D. Chatterjee, D. Bahadur, D. Maiti and S. K. Maji, *J. Mater. Chem. A*, 2019, DOI: 10.1039/C8TA11134K.

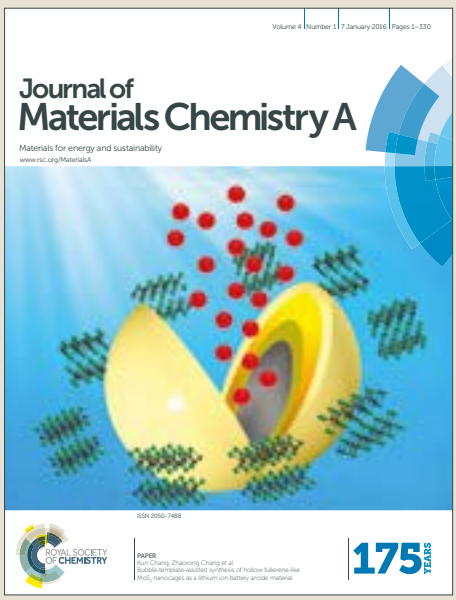

ROYAL SOCIETY OF CHEMISTRY

rsc.li/materials-a

View Article Online
DOI: 10.1039/C8TA11134K

Journal Name

ARTICLE

Fabrication of amyloid fibril-palladium nanocomposite: A sustainable catalyst for C–H activation and electrooxidation of ethanol

Received 00th January 20xx,
Accepted 00th January 20xx

DOI: 10.1039/x0xx00000x

www.rsc.org/

Ramasamy Jayarajan,[†ab] Rakesh Kumar,[†b] Jagriti Gupta,[c] Gayathri Dev,[a] Pradeep Kadu,[b] Debdeep Chatterjee,[b] Dhirendra Bahadur,[c] Debabrata Maiti*[a] and Samir K. Maji*[b]

Amyloids are highly ordered nanofibril and its tensile strength is similar to that of steel, which makes them resistant to extreme *pH* and temperature. Based on this rationale, we demonstrate a facile synthesis of palladium (Pd), copper (Cu), platinum (Pt), gold (Au) and silver (Ag) nanocomposites using α-Synuclein (α-Syn) fibrils as a template. We showed that α-Syn-fibril palladium nanoparticles (α-Syn-PdNPs) composite can be used as a heterogeneous catalyst in C–H bond activation and electrooxidation of ethanol. The study demonstrated α-Syn-PdNPs as a superior heterogeneous catalyst for the synthesis of pharmaceutically valuable benzofuran, naphthofuran, coumarin and *N*-arylindole *via* C–H activation. Further electrooxidation of ethanol using α-Syn-PdNPs displayed an electrochemical active surface area of 160.6 m^2/g, which is much higher than the reported supported Pd nanocomposites.

Introduction

Amyloid fibrils are protein/peptide aggregates consist of cross-β -sheet rich secondary structure.[1] Although, amyloids are mostly associated with human diseases,[1-2] recent studies however suggested that amyloid could do normal physiological functions in host organisms.[2a,3] For example, pMel amyloids are used for templating the melanin polymerization inside the mammalian melanosomes.[3b] Amyloids are highly stable protein fibrils, whose tensile strength is similar to steel[4] and resistant against various harsh environmental conditions such as extreme *pH* and temperature.[5] These properties caught attention of researchers to explicate amyloid based novel biomaterials.[6] In the recent past, Mezzenga and co-workers have actively engaged in the development of amyloid based composites for different applications. These include β-lactoglobulin amyloid as a template for Au as fluorescence material,[7] Au and Pd nanoparticles for continuous flow catalysis,[8] hybrid composite with activated carbon for water purification[9] and gold nanocomposite for aerogel.[10] Further, amyloid iron (Fe) nanoparticles was synthesized and it was shown to be bioavailable.[11] In addition, many studies have reported the application of amyloids and their metal composites, for example building conductive metal nanowires,[12] nanocomposites for optoelectronics and LED applications.[12b,13] Amyloids have also been demonstrated to be a suitable substrate for cell adhesion, drug delivery and tissue engineering applications.[14]

Among various transition metals, Pd-catalysts proved to be privileged in activation of inert C–H bonds over the last decades.[15] Almost every available form of Pd has been exploited in homogeneous catalysis, where the catalyst is often expensive with low recoverability/recyclability.[15c,16] In contrast, a heterogeneous catalytic strategy is inherently promising, since it allows an easier recovery and reuse of catalyst.[17] The supported Pd nanoparticles (PdNPs) found widespread applications in catalysis mostly for classical C–C coupling reactions, due to narrow size distribution, large surface area and high stability.[17c,18] However, the heterogeneous catalysis on C–H functionalization is currently on the verge of exploration.[19]

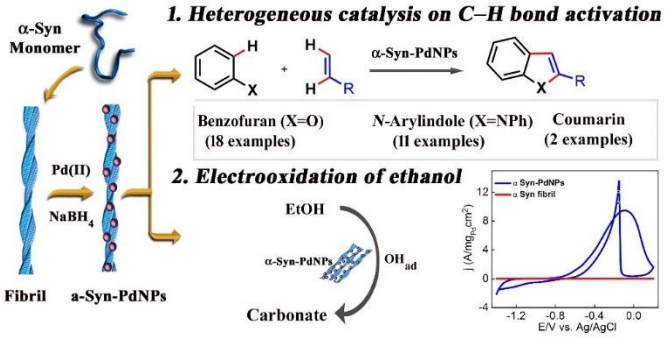

Fig. 1 Synthesis and application of α-Syn-PdNPs. Two applications are shown, one for chemical reactions involving C–H bond activation and another for electrooxidation of ethanol.

Benzofuran and indole core structures exhibit a multitude of pharmaceutical and industrial applications.[20] A simplest

[a] Dr. R. Jayarajan, G. Dev, Prof. Dr. D. Maiti
Department of Chemistry, Indian Institute of Technology Bombay
Powai, Mumbai-400 076 (India). E-mail: dmaiti@chem.iitb.ac.in
[b] Dr. R. Jayarajan, R. Kumar, P. Kadu, D. Chatterjee, Prof. Dr. S. K. Maji, Department of Biosciences and Bioengineering, IIT Bombay. E-mail: samirmaji@iitb.ac.in
[c] J. Gupta, Prof. Dr. D. Bahadur
Department of MEMS, IIT Bombay.
[†] These authors contributed equally to this work

Electronic Supplementary Information (ESI) available: DOI: 10.1039/x0xx00000x

View Article Online
DOI: 10.1039/C8TA11134K

retrosynthetic disconnection path has always caught the attention of synthetic chemistry community.[21] Design of supported PdNPs as a heterogeneous catalyst with high performance for C–H functionalization still remains a great challenge. Further, developing Pd-based direct ethanol fuel cells is an attractive greener strategy, where the support plays a vital role in its enhanced electrocatalytic activity, and superior stability.[22] Choice of supporting material for PdNPs has always been crucial, since the interaction between support and Pd can be reflected in their catalytic behavior and durability.[8] Although, synthesis and various applications of amyloid templated metal composites are well studied,[11,13,23] the application of amyloid templated Pd nanocomposite as a heterogeneous catalyst in C–H activation and electrooxidation of ethanol is not explored. In this study, we demonstrate the synthesis of palladium (Pd), copper (Cu), platinum (Pt), gold (Au) and silver (Ag) nanocomposites using α-Syn-fibrils as a support. Detailed spectroscopic studies on selected nanocomposite, α-Syn-PdNPs and its application as a heterogeneous catalyst in C–H bond activation and electrooxidation of ethanol have been described (Fig. 1).

Results and Discussion

Synthesis and characterization of amyloid-metal nanocomposite

Initially, we expressed and purified α-Syn monomer from *E.coli* and it was used for the synthesis of fibrils. The fibril formation was confirmed by high thioflavin T binding (amyloid fibril specific dye),[24] β-sheet structural transition by circular dichroism (CD) spectroscopy (a negative peak at 218nm)[25] and fibrillar morphology by transmission electron microscopy (TEM). To explore the capability of amyloid fibrils as a template in nanoparticle synthesis, we tested five different metal salts such as $Pd(OAc)_2$, $CuSO_4.5H_2O$, $PtCl_4$, $HAuCl_4.3H_2O$ and $AgNO_3$ in presence of α-Syn-fibrils.[25]

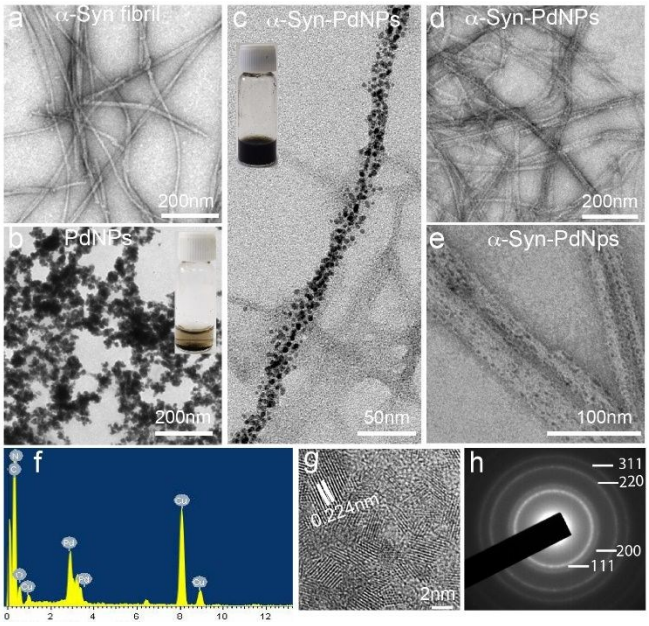

Fig. 2 TEM characterizations of α-Syn-PdNPs. a) Morphology of α-Syn-fibrils. b) Cluster of aggregates observed, when reduction of Pd salt in the absence of fibrils. c) Single amyloid fibril uniformly decorated with PdNPs. d, e) Morphology in different magnification showing highly coated PdNPs along with amyloid fibrils. f) Energy dispersive X-ray spectroscopy profile. g) The lattice fringes showing spacing of 0.224 nm corresponding to the (111) planes in metallic Pd. h) Electron diffraction pattern.

The TEM images of α-Syn-fibrils supported Pd, Cu, Pt, Au and Ag nanoparticles showed highly coated nanoparticles along the fibril length (Fig. S7).[25] Selected area electron diffraction (SAED) pattern of all metal nanocomposites suggested face-centered cubic (fcc) crystal structure.[26] Size of the nanoparticles were found to be *ca*. 2.8 nm for Pd, *ca*. 3 nm for Cu, *ca*. 2.5 nm for Pt, *ca*. 4 nm for Au, and *ca*. 4.4 nm for Ag, respectively (Fig. S7).[25]

Owing to the synthetic and electrochemical applications of Pd-based materials, we chose to study the structural and functional properties of α-Syn-PdNPs in detail. However, the detailed study and possible application of other nanocomposites (Cu, Pt, Au and Ag) would be our future interest. The TEM of α-Syn-fibril and PdNPs alone are shown in Fig. 2a and 2b. The reduction of Pd salt in the absence of fibrils showed a cluster of aggregates (Fig. 2b). A typical single amyloid fibril decorated with PdNPs is depicted in Fig. 2c, which showed a uniform diameter of *ca*. 16 nm. The low-magnification TEM image reveals abundant 1D α-Syn-PdNPs with several micrometer lengths and the mean size of PdNPs was found to be 2.87 nm (Fig. 2d and 2e). Energy dispersive X-ray spectroscopy showed the presence of Pd as a major constituent, whereas oxygen, carbon, and nitrogen represent the key elements of amyloid fibrils (Fig. 2f). The HR-TEM lattice spacing of PdNPs is found to be 0.224 nm, which is consistent with (111) plane of metallic Pd (Fig. 2g).[27] The SAED pattern of PdNPs also confirmed the fcc structure (Fig. 2h). Line mapping of the composite revealed the presence of PdNPs on surface of the fibril (Fig. S8).[25]

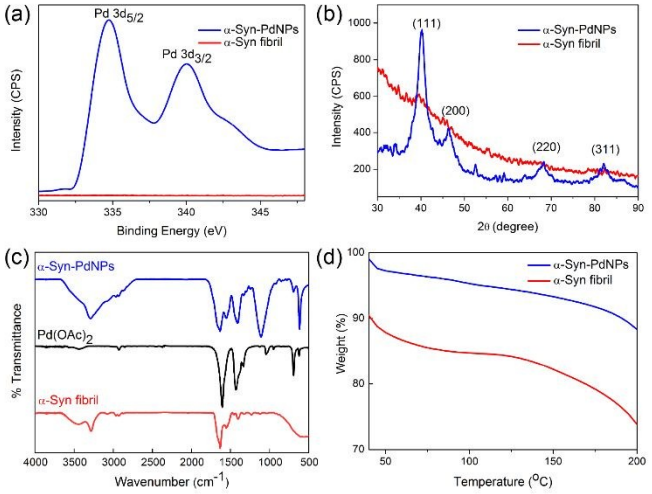

Fig. 3 Spectroscopic characterization of α-Syn-PdNPs. a) XPS resolved spectrum shows two peaks at 334.8 eV and 340.02 eV corresponding to $Pd3d_{5/2}$ and $Pd3d_{3/2}$ respectively. b) Four peaks in powder-XRD pattern reveal the fcc lattice structure of Pd. c) FTIR spectra of α-Syn-fibril, $Pd(OAc)_2$ and α-Syn-PdNPs. d) Thermogravimetric analysis in the temperature range of 25 °C to 200 °C.

The chemical state of PdNPs in the composite was studied by X-ray photoelectron spectroscopy (Fig. S9a).[25] Resolved XPS spectrum showed two peaks; one at 334.8 eV and another at 340.02 eV corresponding to $Pd3d_{5/2}$ and $Pd3d_{3/2}$ respectively (Fig. 3a), that confirms the zero oxidation state of Pd.[17a] The X-ray diffraction pattern clearly displayed four peaks at (111), (200), (220) and (311)

DOI: 10.1039/C8TA11134K

representing the fcc lattice structure of Pd (Fig. 3b, JCPDS 00–005-0681).[28] To study the interaction between the α-Syn-fibril and PdNPs, FTIR analysis was carried out (Fig. 3c). The peak at ~3451 cm^{-1} in the α-Syn-fibril can be assigned for N–H stretching present in the peptide. The broadening of that peak in α-Syn-PdNPs is due to the interaction of N–H with PdNPs.[28] Thermal stability of composite was analyzed by thermogravimetric analysis (Fig. S9b).[25] The spectra recorded from 25 °C to 200 °C temperature is presented, as the chemical reaction was carried out at 110 °C and 130 °C for C–H activation by using this nanocomposite. The results showed the thermal durability of α-Syn-PdNPs, however a slight weight loss has been observed (Fig. 3d).

Heterogeneous catalysis on C–H activation using α-Syn-PdNPs

After unambiguous characterization, we explored the activity of α-Syn-PdNPs as heterogeneous catalyst in the organic reactions involving C–C, C–O/C–N bond formation *via* triple C–H bond activation, which is previously performed through homogeneous fashion with $Pd(OAc)_2$.[21b] The amount of Pd in the composite was estimated to be 20 wt% by inductively coupled plasma atomic emission spectroscopy (ICP-AES) measurement.[25] During initial exploration, the reaction was performed between 4-nitrophenol and styrene using 5 mol% of α-Syn-PdNPs as a catalyst, 10 mol% of 1,10-phenanthroline, 1 equiv of $Cu(OAc)_2.H_2O$ and 3 equiv of NaOAc at 110 °C in dichloroethane (DCE) as a solvent.[21b] The reaction produced only 12% of benzofuran product (Table S3).[25] The low yield is likely due to the inefficiency of $Cu(OAc)_2.H_2O$ in the oxidation of Pd(0) to Pd(II) in the initial step under reaction conditions. Use of 1,4-benzoquinone (1 equiv) as an oxidant, however, provided slightly improved yield (28%) (Table S3).[25] Among various oxidants, V_2O_5 resulted in the improved yield of 48%. After an extensive optimization of reaction conditions, excellent yield of product 5-nitro-2-phenylbenzofuran **4a** (91%) was achieved from 4-nitrophenol and styrene, using α-Syn-PdNPs (7.5 mol%), 1,10-phenanthroline (15 mol%), V_2O_5 (2.5 equiv), and NaOAc (1.5 equiv) in DCE at 110 °C for 24 hours (Table S3-S10).[25] This reaction, therefore, suggests that along with catalyst, the use of base and ligand plays a significant role in the reaction.

Proceeding further with the optimized condition, we probed scope of the reaction with various substituted phenols and styrenes (Table 1). *Meta* or *para* substituted styrenes were also well reacted with 4-nitrophenol and yielded the product in 62-86% (**4b**-**4e**, Table 1). Differently substituted styrenes such as carbonyl (**4g**), sterically encumbered *tert*-butyl (**4h**) and halogen (**4i**) were all well tolerated and delivered the desired product. Switching the electronic nature of the phenol by varying substitution was also tested (**4j**). Halogen substituent at both phenol and styrene also produced benzofuran (**4k**) with 66% yield. Subsequently, we focused on the synthesis of pharmacologically important naphthofuran derivatives.[29] We tested 2-naphthol derivatives with electron withdrawing and donating substituent on the styrene. All reactions successfully yielded 2-arylnaphthofuran derivatives **4l**-**4o** (Table 1).

Use of aliphatic olefins such as cyclohexene or allyl chloride as a coupling partner with 4-nitrophenol provided fused benzofuran derivative (**4p**) or 2-methyl-7-arylbenzofuran (**4q**), respectively with good yields. Allyl bromide with 6-bromonaphthol gave desired naphthofuran derivative (**4r**). Next, we tested coumarin synthesis by reacting 4-nitro/methoxy phenol with methyl acrylate (**4s** and **4t**, Table 1) under slightly modified conditions.[25]

Table 1. Synthesis of benzofuran, naphthofuran, coumarin and *N*-arylindole *via* C–H activation using amyloid supported PdNPs as a heterogeneous catalyst

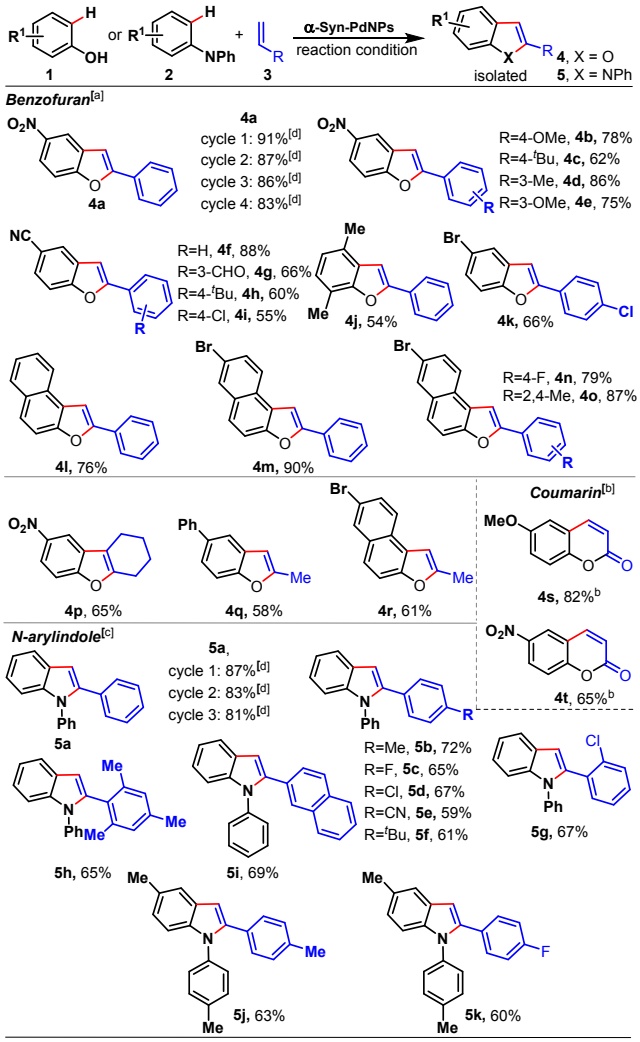

[a]Reaction conditions: **1** (1 mmol) and **3** (0.5 mmol), α-Syn-PdNPs (7.5 mol%), 1,10-phenanthroline (15 mol%), V_2O_5 (2.5 equiv), NaOAc (1.5 equiv), $ClCH_2CH_2Cl$ at 110 °C for 24 h; [b] **1** (1 mmol) and ethylacrylate (0.5 mmol), α-Syn-PdNPs (10 mol%), 1,10-phenanthroline (20 mol%), V_2O_5 (2.5 equiv), NaOAc (1.5 equiv), MS (4Å, 130 mg), $ClCH_2CH_2Cl$ at 110 °C for 24 h; [c] **2** (1 mmol) and **3** (0.25 mmol), α-Syn-PdNPs (10 mol%), 1,10-phenanthroline (20 mol%), CuOAc (2 equiv), $ClCH_2CH_2Cl$ at 130 °C for 24 h; [d]Refer Supporting Information.[25]

We further tested α-Syn-PdNPs in the synthesis of *N*-arylindoles by direct reaction between *N*,*N*-diarylamines and olefins (Table 1).[21a] Initial reaction between diphenylamine and styrene in acetic acid gave 30% yield of the desired product (Table S11).[25] Considering the recoverability of the catalyst, we intended to find an alternate solvent. Thus, the reaction condition was extensively optimized to obtain the desired *N*-arylindole in synthetically useful yield (Table S11-S16).[25] The highest synthetic yield of product, 1,2-diphenyl-1H-indole **5a** (87%) was obtained under optimized condition of

DOI: 10.1039/C8TA11134K

diphenylamine (1 equiv), styrene (0.25 equiv), α-Syn-PdNPs (10 mol%), 1,10-phenanthroline (20 mol%) and CuOAc (2 equiv) in DCE at 130 °C for 24 h (Table S15).[25] To explore the feasibility of the optimized reaction conditions, substituted diphenylamines and styrenes were exploited to get the desired 2-aryindole products (**5b**-**5k**, Table 1).

Since amyloid fibrils are insoluble, we hypothesized that α-Syn-PdNPs can repeatedly be isolated by centrifugation after each reaction cycle. The recyclability of the catalyst was examined for both benzofuran and *N*-arylindole synthesis under standard reaction conditions.[25] The calculated turnover number (TON) with the use of 7.5 mol% catalyst (α-Syn-PdNPs) loading for the benzofuran (**4a**) synthesis is ~13 (12.67). Catalytic activity remained nearly unaffected up to four reaction cycles in benzofuran (**4a**, Table 1) and three cycles in *N*-arylindole (**5a**, Table 1) synthesis, respectively. TEM was recorded for the recovered composite up to four cycles in benzofuran and after the third cycle in *N*-arylindole synthesis (Fig. S6 and S11). A slight change in morphology of amyloid fibril was observed, however, PdNPs were intact on the fibril surface. Interestingly the size of the Pd nanoparticle size distributions is mostly unchanged even after four cycle of the reaction suggesting durability and integrity of the catalyst (Table S1 and Fig. S6).[25] Further CD spectra for both α-Syn fibril as well as the nanocomposite (α-Syn-PdNPs) showed a negative peak at 218 nm, which can be assigned for the β-sheet structure of the fibril.[30a-c] Similar trend has been observed for a recovered α-Syn-PdNPs (after four cycle) with a slightly reduced intensity. This data suggest that α-Syn fibril structure is mostly unaffected even after four cycle of chemical reaction.

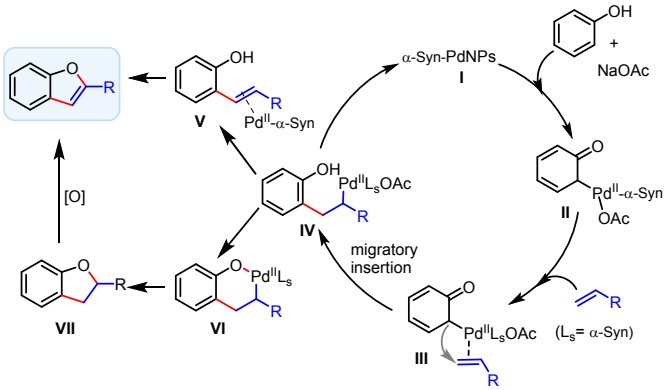

Scheme 1. Plausible catalytic cycle for α-Syn-PdNPs catalyzed synthesis of benzofuran

The plausible catalytic cycle for α-Syn-PdNPs catalyzed formation of benzofuran have been described in Scheme 1.[21b] In the first step, palladium catalyst **I** (α-Syn-PdNPs) inserts at the *ortho* position of phenol and can provide the quinone-type intermediate (**II**). The Pd(0) coordination with oxygen atom of phenol is unlikely according to hard and soft acids and bases (HSAB) principle.[31a] The most likely conjugate base of phenol (hard base) might not coordinate to the Pd(0); whereas the *ortho* carbon of phenol-a soft base can apparently form a bond with Pd(II), which is a soft acid. Olefin coordination at Pd center of intermediate **II** leads to intermediate **III** and migratory insertion of olefin *via* sterically less hindered carbon can lead to intermediate **IV**.[31b] Subsequent steps can provide intermediate **V** or **VI**, which can be converted into the benzofuran **4**. A similar type of catalytic cycle can be followed for the synthesis of *N*-arylindole **5** (Scheme S1).[25]

Table 2. Screening of different catalysts[a]

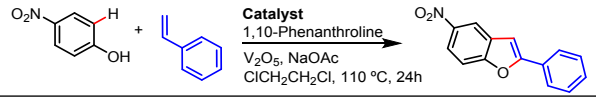

Entry	Catalyst	Yield[b]
1	α-Syn monomer-PdNPs	50
2	Sonicated α-Syn-PdNPs	65
3	Proteinase k digested α-Syn-PdNPs	30
4	PdNPs supported on fibrous silica, (KCC-1-PEI/Pd)[30] (10 mol%)	20
5	PdNPs supported on fibrous silica, (KCC-1-PEI/Pd)[30] (20 mol%)	35
6	PdNPs alone (unsupported)	57
7	α-Syn fibril alone	0
8	PdNPs (7.5 mol%) + α-Syn fibril (5 mg)	58
9	PdNPs (7.5 mol%) + α-Syn fibril (10 mg)	55
10	**α-Syn-PdNPs**	**95**

[a]Reaction conditions: 4-nitrophenol (1 mmol) and styrene (0.5 mmol), catalyst (7.5 mol%), 1,10-phenanthroline (15 mol%), V_2O_5 (2.5 equiv), NaOAc (1.5 equiv), $ClCH_2CH_2Cl$ at 110 °C for 24 h; [b]Yields were calculated by GC using n-decane as internal standard.

To study the role of amyloid fibril as a support in catalytic performance, we carried out the control experiments by varying morphology of the α-Syn-fibril (Fig. S10),[25] with previously reported fibrous silica supported PdNPs (KCC-1-PEI/Pd),[30d] unsupported PdNPs, α-Syn-fibril alone and mixture of both α-Syn-fibril and PdNPs (entries 1-9, Table 2). Excellent yield of the product was observed only when intact α-Syn-fibril was used as support compared to others (entry 10, Table 2). The relatively low yields were obtained when the reaction carried out with a physical mixture of PdNPs and α-Syn fibrils (entries 8-9, Table 2). These results suggest that catalyst synthesized with α-Syn fibril template possess higher catalytic efficiency.

Electrooxidation of ethanol using α-Syn-PdNPs

Previous reports demonstrated electrooxidation of alcohol using Pd or Pt nanoparticles with different supporting materials such as metals, metal alloys, reduced graphene oxide and insulin amyloid fibrils.[17a,22c,26,32] We explored the electrocatalytic activity of α-Syn-PdNPs towards electrooxidation of ethanol. Initially the cyclic voltammetry (CV) measurements were carried out for α-Syn-PdNPs in 1 M KOH solution (without ethanol) at the scan rate of 50 mVs^{-1}, to examine the electrochemical property and stability (Fig. 5a-c). The Fig. 5a shows one peak in the anodic scan (forward scan) at potential −0.59 V, which is associated with the formation of adsorbed OH^- and desorption of hydrogen on the Pd surface.[32a] In the backward scan, two peaks were observed; one peak in the cathodic scan at potential −0.38 V, which is associated with the reduction of PdO to metallic Pd and another peak at potential −0.83 V is related to hydrogen adsorption.[17a] Important to note that the reduction of PdO to metallic Pd is not only an electron transfer event, but might also be a bond breaking reaction that involves in the release of OH^-. The plausible reaction mechanism is discussed in Supporting Information.[33]

View Article Online
DOI: 10.1039/C8TA11134K

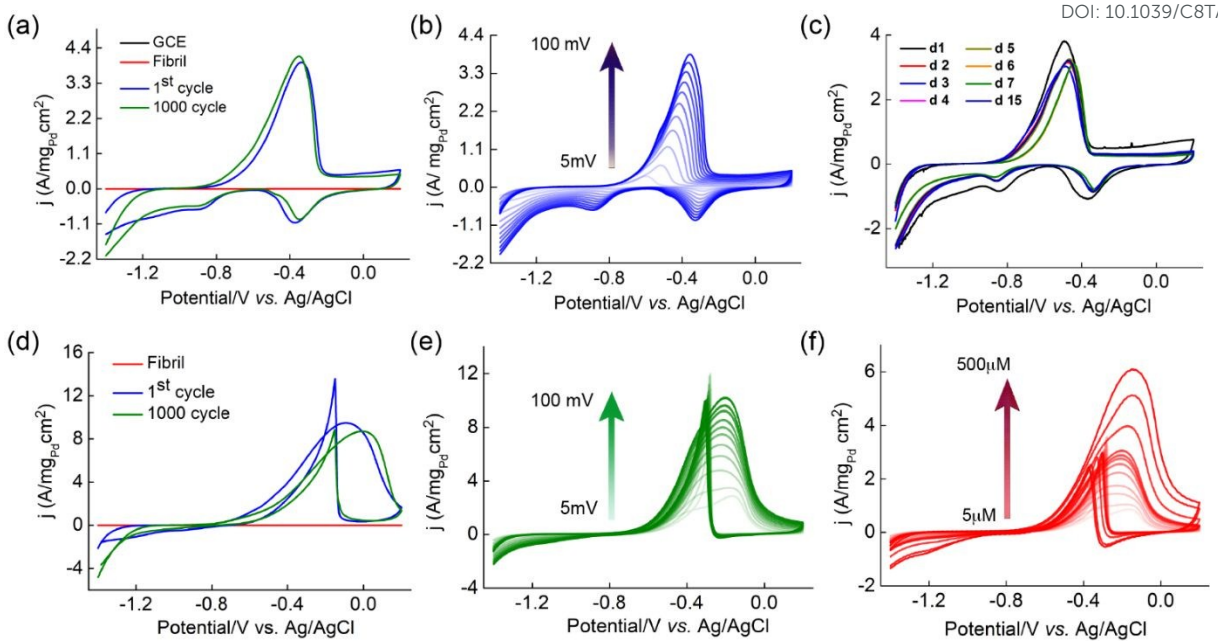

Fig. 5 a) Cyclic voltammograms (CVs) of α-Syn-fibril and α-Syn-PdNPs on GCE in 1 M KOH at the scan rate of 50 mV s^{-1}. b) CVs of α-Syn-PdNPs in 1 M KOH with varying scan rate. c) CVs of day wise experiment with α-Syn-PdNPs in 1 M KOH at the scan rate of 50 mV s^{-1} d) CVs of α-Syn-fibril and α-Syn-PdNPs in 1 M KOH + 1 M ethanol at the scan rate of 50 mV s^{-1} up to 1000 cycles. e) Current density changes with varying scan rate in 1 M KOH + 1 M ethanol. f) CVs of α-Syn-PdNPs in 1 M KOH with various concentration of ethanol at the scan rate of 50 mV s^{-1}.

It was observed that the mass current density increases with increased scan rate and shape of CVs exhibit a relatively reversible electrochemical reaction (Fig. 5b). This makes a sufficient fast electron transfer rate for good electrochemical performance. The α-Syn-PdNPs showed excellent electrochemical performance at all scan rate and higher stability up to 1000 cycles as well as in day wise study (Fig. 5c). The calculated electrochemical active area (ECSA) of the α-Syn-PdNPs composite was found to be 160.6 m^2/g, which is higher than the other reported Pd-based nanocomposite (Table S2).[25] Higher ECSA indicates that composite have higher active catalytic surface area with higher number of catalytically active sites, which are essential for electrochemical oxidation of ethanol.

The electrocatalytic activity of α-Syn-PdNPs for electrooxidation of ethanol (EOR) was investigated in KOH (1 M) and ethanol (1 M) at scan rate of 50 mV s^{-1} (Fig. 5d), which shows two well-defined characteristic current peaks in the forward and reverse potential windows. The first peak in the forward direction (positive scan) corresponds to the ethanol oxidation; while the second peak in the reverse scan attributes to the oxidation of freshly adsorbed ethanol and adsorbed carbonaceous species.[22c] The current in the reverse scan is quite sharp, that reveals a significant oxidation of adsorbed intermediate species on the highly active α-Syn-PdNPs composite. This implies that the ethanol oxidation could not be occurring directly through a total oxidation to CO_2.[22b,32a] However, no current density peak is observed for α-Syn-fibril alone indicating that fibril is inactive for ethanol oxidation. Long-term stability of α-Syn-PdNPs towards ethanol oxidation was observed up to 1000 cycles, wherein only 8% loss occurs in the mass current density (Fig. 5d). The mass peak current density of forward scan of the composite is 9.4 A/mgPd cm^2, which is much higher than the reported Pd-based nanocomposites (Table S2).[25] Further, investigation by varying scan rate showed an increase in current density with increased scan rate (Fig. 5e). We have carried out GC and NMR studies to identify the products or intermediate species formed during electrooxidation of ethanol (after 1000 cycles). Although the accurate quantification of products or intermediate is tricky, the analyzed spectral data revealed the presence of compounds such as acetic acid and polymeric species of acetaldehyde; paraldehyde (Fig. S2-S4).[25] This confirms the oxidation of ethanol occurred during CV experiments. Further, the plausible intermediate formation during electrooxidation of ethanol has been discoursed in Supporting Information.[34]

The effect of ethanol concentration on EOR was further analyzed (Fig. 5e). The results show that the mass current densities increase with ethanol concentration from 5 to 500 µM as well as peak potential (Ep) shifted towards more positive potentials. Therefore, it was presumed that OH^- adsorption is independent of ethanol concentration. Moreover, when the ethanol concentration increases, the surface area of Pd nanocomposite covered by ethoxy species gradually increased, which leads to higher current densities. Furthermore, to compute the tolerance of α-Syn-PdNPs towards EOR, chronoamperometry at different potentials were performed in KOH (1 M) + ethanol (1 M) up to 1000 seconds (Fig. 6). The chronoamperometry results showed that α-Syn-PdNPs exhibits a rapid decrease in the current density at the beginning, indicating the formation of carbonaceous intermediates during the ethanol oxidation, which then remains constant (Fig. 6).[25] The higher current density was observed with α-Syn-PdNPs at the start and end of the tests, signifying its superior catalytic activity and durability against the poisoning. Overall, the enhanced activity of the present Pd nanocomposite is due to the number of abundant Pd nanoparticle and its activity improvement on the active sites, which can be ascribed to the strong interactions between the amyloid and Pd nanoparticles.

The amino acid sequences that present in the amyloid might provide homing to PdNPs, which can concurrently probe the electronic behavior of PdNPs towards high catalytic efficiency. Furthermore, amyloids known to possess unique combination of both hydrophobic and hydrophilic surfaces, which enable amyloid to interact with wide ranges of small molecules, polymers and proteins.[14b,35] These unique surfaces of amyloids not only enhance the formation of uniform PdNPs that might possess high catalytic efficiency but may also help substrate to localize on the catalyst surface.

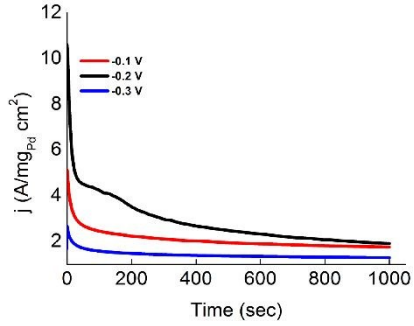

Fig. 6. Chronoamperogram with varying potential in 1 M KOH + 1 M ethanol at the scan rate of 50mV s-1.

Conclusions

The present work revealed the use of newly developed nanostructured amyloid templated Pd nanoparticles (α-Syn-PdNPs) as an excellent heterogeneous catalyst for the synthesis of biologically valuable heterocycles such as benzofuran, naphthofuran, coumarin and *N*-arylindole *via* C–H bond activation strategy. The superior electrocatalytic performance of α-Syn-PdNPs on the electrooxidation of ethanol further enhances its utility as a catalyst for the development of potential ethanol fuel cells. These enhanced activities can be explained based on the unique structural properties and stability of amyloid fibrils, which is essential to grasp the metal nanoparticle under various conditions. Overall merging biomolecular frameworks with metal nanoparticle can further provide unique applications in material science as well as nanobiotechnology.

Conflicts of interest

There are no conflicts to declare.

Acknowledgements

This research activity was supported by DST Nano Mission (SR/NM/NS-1065/2015) India. Financial support from DST-India (R.J.) and MHRD (R.K.) is gratefully acknowledged.

Notes and references

1. S. Mankar, A. Anoop, S. Sen, and S. K. Maji, *Nano Rev.,* 2011, *6032*.
2. (a) F. Chiti and C. M. Dobson, *Annu. Rev. Biochem.,* 2006, **75**, 333-366; (b) M. Stefani and C. M. Dobson, *J. Mol. Med.,* 2003, **81**, 678-699.
3. (a) M. R. Chapman, L. S. Robinson, J. S. Pinkner, R. Roth, J. Heuser, M. Hammar, S. Normark and S. J. Hultgren, *Science,* 2002, **295**, 851-855; (b) D. M. Fowler, A. V. Koulov, C. A. Jost, M. S. Marks, W. E. Balch and J. W. Kelly, *PLoS Biol.,* 2006, **4**, e6.
4. J. F. Smith, T. P. Knowles, C. M. Dobson, C. E. Macphee and M. E. Welland, *Proc. Natl. Acad. Sci. U.S.A.,* 2006, **103**, 15806-15811.
5. T. P. Knowles, A. W. Fitzpatrick, S. Meehan, H. R. Mott, M. Vendruscolo, C. M. Dobson and M. E. Welland, *Science,* 2007, **318**, 1900-1903.
6. (a) S. Padalkar, J. Hulleman, P. Deb, K. Cunzeman, J. C. Rochet, E. A. Stach and L. Stanciu, *Nanotechnology* 2007, **18**, 055609; (b) R. Colby, J. Hulleman, S. Padalkar, J. C. Rochet and L. A. Stanciu, *J. Nanosci. Nanotechnol.,* 2008, **8**, 973-978.
7. S. Bolisetty, J. J. Vallooran, J. Adamcik, S. Handschin, F. Gramm and R. Mezzenga, *J. Colloid Interface Sci.,* 2011, **361**, 90-96.
8. S. Bolisetty, M. Arcari, J. Adamcik and R. Mezzenga, *Langmuir,* 2015, **31**, 13867-13873.
9. S. Bolisetty and R. Mezzenga, *Nat. Nanotechnol.,* 2016, **11**, 365-371.
10. G. Nystrom, M. P. Fernandez-Ronco, S. Bolisetty, M. Mazzotti and R. Mezzenga, *Adv. Mater.,* 2016, **28**, 472-478.
11. Y. Shen, L. Posavec, S. Bolisetty, F. M. Hilty, G. Nystrom, J. Kohlbrecher, M. Hilbe, A. Rossi, J. Baumgartner, M. B. Zimmermann and R. Mezzenga, *Nat. Nanotechnol.,* 2017, **12**, 642-647.
12. (a) M. Reches and E. Gazit, *Science,* 2003, **300**, 625-627; (b) T. Scheibel, R. Parthasarathy, G. Sawicki, X. M. Lin, H. Jaeger and S. L. Lindquist, *Proc. Natl. Acad. Sci. U.S.A.,* 2003, **100**, 4527-4532.
13. (a) I. Cherny and E. Gazit, *Angew. Chem. Int. Ed.,* 2008, **47**, 4062-4069; T. P. Knowles and R. Mezzenga, *Adv. Mater.,* 2016, **28**, 6546-6561.
14. (a) D. S. Benoit, A. R. Schwartz, M. P. Durney, K. S. Durney, A. R. Anseth and K. S. Anseth, *Nat. Mater.,* 2008, **7**, 816-23; (b) S. Das, R. S. Jacob, K. Patel, N. Singh and S. K. Maji, *Biomacromolecules* 2018, **19**, 1826-1839.
15. (a) L. Ackermann, R. Vicente and A. R. Kapdi, *Angew. Chem. Int. Ed.,* 2009, **48**, 9792-9826; (b) S. Murai, F. Kakiuchi, S. Sekine, Y. Tanaka, A. Kamatani, M. Sonoda and N. Chatani, *Nature,* 1993, **366**, 529-531; (c) H. P. L. Gemoets, I. Kalvet, A. V. Nyuchev, N. Erdmann, V. Hessel, F. Schoenebeck and T. Noel, *Chem. Sci.,* 2017, **8**, 1046-1055; (d) N. Kuhl, M. N. Hopkinson, J. W. Delord and F. Glorius, *Angew. Chem. Int. Ed.,* 2012, ***51***, 10236-10254.
16. (a) L. Ackermann and A. Althammer, *Angew. Chem. Int. Ed.,* 2007, **46**, 1627-1629; (b) N. Erdmann, Y. Su, B. Bosmans, V. Hessel and T. Noel, *Org. Process Res. Dev.,* 2016, **20**, 831-835.
17. (a) S.-H. Ye, J.-X. Feng and G.-R. Li, *ACS Catal.,* 2016, **6**, 7962-7969; (b) F. Ferlin, S. Santoro, L. Ackermann and L. Vaccaro, *Green Chem.,* 2017, **19**, 2510-2514; (c) D. Rasina, A. Kahler-Quesada, S. Ziarelli, S. Warratz, H. Cao, S. Santoro, L. Ackermann and L. Vaccaro, *Green Chem.,* 2016, **18**, 5025-5030.
18. (a) A.-L. Wang, X.-J. He, X.-F. Lu, H. Xu, Y.-X. Tong and G.-R. Li, *Angew. Chem. Int. Ed.,* 2015, **54**, 3669-3673; (b) X. Tian, F. Yang, D. Rasina, M. Bauer, S. Warratz, F. Ferlin, L. Vaccaro and L. Ackermann, *Chem. Comm.,* 2016, **52**, 9777-9780; (c) M. E. Martinez-Klimov, P. Hernandez-Hipolito, M. Martinez-Garcia and T. E. Klimova, *Catal. Today*, 2018, **305**, 58-64; (d) Y. Yan, J. Miao, Z. Yang, F.-X. Xiao, H. B. Yang, B. Liu and Y. Yang, *Chem. Soc. Rev.*, 2015, **44**, 3295-3346; (e) A. Taher, M. Choudhary, D. Nandi, S. Siwal and K. Mallick, *Appl. Organometal. Chem.*, 2018, **32**, e3898.
19. (a) L. Djakovitch and F.-X. Felpin, *ChemCatChem* 2014, **6**, 2175-2187; (b) S. Korwar, M. Burkholder, S. E. Gilliland III, K. Brinkley, B. F. Gupton and K. C. Ellis, *Chem. Commun*., 2017, **53**, 7022-7025; (c) A. J. Reay and I. J. S. Fairlamb, *Chem. Commun*., 2015, **51**, 16289-16307; (d) S. Korwar, K. Brinkley, A. R. Siamaki, B. F.

View Article Online
DOI: 10.1039/C8TA11134K

Gupton, and K. C. Ellis, *Org. Lett.* 2015, **17**, 1782-1785; (e) S. Santoro, S. I. Kozhushkov, L. Ackermann and L. Vaccaro, *Green Chem.,* 2016, **18**, 3471-3493;

20. (a) H. Tsuji, C. Mitsui, L. Ilies, Y. Sato and E. Nakamura, *J. Am. Chem. Soc.,* 2007, **129**, 11902-11903; (b) A. J. Kochanowska-Karamyan, M. T. Hamann, *Chem. Rev.,* 2010, **110**, 4489-4497.
21. (a) U. Sharma, R. Kancherla, T. Naveen, S. Agasti and D. Maiti, *Angew. Chem. Int. Ed.,* 2014, **53**, 11895-11899; (b) U. Sharma, T. Naveen, A. Maji, S. Manna and D. Maiti, *Angew. Chem. Int. Ed.,* 2013, **52**, 12669-12673.
22. (a) S. Ghosh, H. Remita, P. Kar, S. Choudhury, S. Sardar, P. Beaunier, P. S. Roy, S. K. Bhattacharya, S. K. Pal, *J. Mater. Chem. A,* 2015, ***3***, 9517-9527; (b) C. W. Xu, H. Wang, P. K. Shen, S. P. Jiang, *Adv. Mater.,* 2007, **19**, 4256-4259; (c) X. Chen, Z. Cai, X. Chen, M. Oyama, *J. Mater. Chem. A,* 2014, **2**, 315-320.
23. G. Wei, Z. Su, N. P. Reynolds, P. Arosio, I. W. Hamley, E. Gazit and R. Mezzenga, *Chem. Soc. Rev.,* 2017, **46**, 4661-4708.
24. LeVine, H., 3rd, *Methods Enzymol,* 1999, **309**, 274-284.
25. See Supporting Information for detailed desciption.
26. L. Zhang, N. Li, F. Gao, L. Hou and Z. Xu, *J. Am. Chem. Soc.,* 2012, **134**, 11326-11329.
27. G. Zhu, Y. Jiang, W. Huang, H. Zhang, F. Lin and C. Jin, *Chem. Comm.,* 2013, **49**, 10944-10946.
28. S. Yang, J. Dong, Z. Yao, C. Shen, X. Shi, Y. Tian, S. Lin, X. Zhang, *Sci. Rep.,* 2014, **4**, 4501.
29. R. Le Guével, F. Oger, A. Lecorgne, Z. Dudasova, S. Chevance, A. Bondon, P. Barath, G. Simonneaux and G. Salbert, *Bioorg. Med. Chem.,* 2009, **17**, 7021-7030.
30. (a) D. Ghosh, M. Mondal, G. M. Mohite, P. K. Singh, P. Ranjan, A. Anoop, S. Ghosh, N. N. Jha, A. Kumar and S. K. Maji, *Biochemistry* 2014, **53**, 6419-6421; (b) S. Maji, L. Wang, J. Greenwald and R. Riek, *FEBS Lett*., 2009, **583**, 2610-2617; (c) W. Curtis Johnson, Jr. *Ann. Rev. Biophys. Biophys. Chern.,* 1988, **17**, 145-156. (d) P. K. Kundu, M. Dhiman, A. Modak, A. Chowdhury, V. Polshettiwar and D. Maiti, *ChemPlusChem,* 2016, **81**, 1142-1146.
31. (a) H. Mayr, M. Breugst, and A. R. Ofial, *Angew. Chem. Int. Ed.,* 2011, **50**, 6470-6505; (b) A. Maji, Y. Reddi, R. B. Sunoj, and D. Maiti, *ACS Catal.,* 2018, **8**, 10111-10118.
32. (a) R. Kumar, R. Savu, R. K. Singh, E. Joanni, D. P. Singh, V. S. Tiwari, A. R. Vaz, E. T. S. G. da Silva, J. R. Maluta, L. T. Kubota and S. A. Moshkalev, *Carbon,* 2017, **117**, 137-146; (b) L. Chen, L. Lu, H. Zhu, Y. Chen, Y. Huang, Y. Li and L. Wang, *Nat. Commun.,* 2017, **8**, 14136; (c) X. Chen, G. Wu, J. Chen, X. Chen, Z. Xie, X. Wang, *J. Am. Chem. Soc.,* 2011, **133**, 3693-3695; (d) F. Ren, H. Wang, C. Zhai, M. Zhu, R. Yue, Y. Du, P. Yang, J. Xu, W. Lu, *ACS Appl. Mater. Interfaces* 2014*,* **6***,* 3607-3614.
33. I. Feliciano-Ramos, E. O. Ortiz-Quiles, L. Cunci, D. C. Díaz-Cartagena, O. Resto and C. R. Cabrera, *J. Solid State Electrochem.*, 2016, **20**, 1011-1017.
34. Y. Wang, S. Zou, W. B. Cai, *Catalysts*, 2015, **5**, 1507-1534.
35. (a) R. S. Jacob, D. Ghosh, P. K. Singh, S. K. Basu,; N. N. Jha, S. Das, P. K. Sukul, S. Patil, S. Sathaye, A. Kumar, A. Chowdhury, S. Malik, S. Sen and S. K. Maji, *Biomaterials***,** 2015, **54**, 97-105; (b) J. Greenwald and R. Riek, *Structure*, 2010, **18**, 1244-1260; (c) R. Schwartz and J. King, *Protein Sci.*, 2006, **15**, 102-112.